Engineering and Technology Journal
Journal homepage: https://etj.uotechnology.edu.iq

Design of Optimal PID Controller for Electric Vehicle Based on Particle Swarm and Multi-Verse Optimization algorithms

Arkan A. Jassim*[a], Ekhlas H. Karam[b], Mohammed Moanes E. Ali[c]

[a] Medical Instruments Engineering Techniques Dept., Bilad Alrafidain University College, 32001 Diyala, Iraq.
[b] Computer Engineering Dept., Mustansiriyah University, Baghdad, Iraq.
[c] Electrical Engineering Dept., University of Technology-Iraq, Alsina'a street, 10066 Baghdad, Iraq.
*Corresponding author Email: arkan199328@gmail.com

HIGHLIGHTS

- A nonlinear dynamic concept of an electric vehicle was developed by fusing kinetic and electrical components.
- A proportional Integral derivative (PID) controller to stay the vehicle on the course was created.
- Particle Swarm Optimization (PSO) and Multi-Verse Optimization (MVO) algorithms are used to obtain optimal parameters for this controller.
- The proposed controllers were tested with linear and nonlinear trajectories to represent the speed of electric vehicles.

ARTICLE INFO

Handling editor: Ivan A. Hashim

Keywords:
Electrical vehicle; PID Controller; Optimization Methods; Particle Swarm Optimization (PSO); Multi-Verse Optimization (MVO).

ABSTRACT

The automotive industry is moving toward more environmentally friendly automobiles with greater range and performance than traditional vehicles as the effects of global warming worsen. Because of the positive impact, electric vehicles can have on reducing harmful emissions from the transportation sector, scientists have grown increasingly interested in the possibility of analyzing and simulating electric vehicles. In this study, we develop a non-linear dynamic concept of an electric vehicle by fusing kinetic and electrical components. Then we create a proportional Integral derivative (PID) controller to help it stay on course. To obtain optimal parameters for this controller by minimizing the error between the desired and actual output, Particle Swarm Optimization (PSO), and Multi-Verse Optimization (MVO) algorithm are used. The proposed controllers tested with linear and nonlinear trajectories to represent the electric vehicle's speed. The computation findings show that the proposed controller works perfectly, keeping up with the electric vehicle's speed quickly and precisely. In particular, the MVO-based proportional-integral-derivative (PID) controller is superior to the proportional-integral-derivative (PID) -based PSO method in terms of no steady-state error and smallest overshoot (0.05% with MVO while 0.25% with PSO) prevention for electric vehicle (EV) speed despite the better results of settling time and rising time obtained in PSO (0.767 And 0.211 s) respectively while these values were (0.807 and 0.215 s), respectively, in MVO. All works are performed in MATLAB (R2020a)/Simulink environment.

1. Introduction

Fuel-engine vehicles with internal composition engines (ICE) are not currently the preferred vehicles; environmental protection awareness has led researchers to search for a cleaner way to transport passengers and reduce pollution Vehicle technologies can effectively reduce fuel use and air pollution [1].

Electric vehicle creates additional opportunities by improving the quality of life, reducing energy spending, and decreasing reliance on foreign oil. The market of Electric vehicles is growing in a big way globally. The demand for this type represents both a challenge and an opportunity to capitalize on new vehicle technology and, in the process, reap substantial economic development [2].

However, the widespread use of electric vehicles faces hindrances due to factors like the limited battery capacity, which cruises between 150km and 200km [3]. Many restrictions are introduced in the travel behavior of electric vehicle drivers due to the driving range limit, because of insufficient coverage of charging station infrastructure in the near future.

The advancement in electric vehicles will lead to some profound changes, including technology, manufacturing systems, distribution and aftermarket service, and support. The manufacturing of Electric vehicles is less complex than that of ICE vehicles due to fewer moving components [4].

http://doi.org/10.30684/etj.2023.135587.1279
Received 30 August 2022; Accepted 01 January 2023; Available online 27 January 2023
2412-0758/University of Technology-Iraq, Baghdad, Iraq

What makes EVs explicitly powerful are the transmission and differential gears of the electric motors. A battery is a source of direct current (DC) power [4]. A DC motor benefits from two main advantages. Primarily, due to its simplicity, it is a robust and cheap technology. Moreover, it provides maximum start-up torque. Like any other system, the electric vehicle must be supplied by power, commanded by the user, controlled to obtain the best performance, and have an actuator to operate [5, 6].

Previously, many kinds of research have been published on the controllers for electric vehicles. In 2015, Xian J. Jin and others presented a gain-scheduled controller for the independent drive of four-wheel electric vehicle lateral stability [7]. In 2017, Ali Pakniyat and others proposed a hybrid framework for electric vehicle control and analysis [8]. In 2018, Nitin K. Saxena and others designed a PI (proportional-integral) based controller for managing electric vehicle battery output voltage [9]. In 2018, Zhengyuan Wang and others proposed a gain-scheduled LQR (Linear Quadratic Regulator) to control the electric vehicle's yaw moment [10]. In 2019, Jemma J. Makrygiorgou and others presented the design of a power controller for the battery operation and the motor of an electric vehicle. The authors used a PI controller for the speed control of the vehicle motor (external loop) and a cascaded PI/P scheme to control the DC voltage/battery and current maintenance, respectively [11]. In 2020 Chih H. Chiu and others designed a fuzzy Type-2 controller for the control of SWV (Single-Wheel Electric Vehicle) [1]. In 2021, K. A. Nitesh et al. presented initial reviews on the different battery packs for Electric Vehicles (EV)/Hybrid EV (HEV), and later, a battery management system was proposed where the State-of-Charge (SoC) is estimated accurately for different battery packs [12]. An optimal improved PID controller is suggested in this paper for a non-linear dynamic model of the electric vehicle. This controller consists of an optimal PID controller with Two Optimization Methods (PSO and MVO). We will explain this controller's details in this paper's sections. Our subsequent paper is structured as follows: Modeling for electric vehicles is discussed in Section 2. In Section 3, we discuss the PID control system that has been developed. Section 4 details optimization methodologies. The section devoted to presenting the results obtained in Section 5. A conclusion is provided in Section 6.

2. Mathematical Model of Electric Vehicles

2.1 The Kinetics of EV

An electric vehicle is depicted in Figure 1 as it is in equilibrium with regard to all of the forces operating upon it when it is in motion. These forces include the traction force and the road load. Trying to roll the reaction of the tires, the force of gravitational influence, the force of aerodynamic drag, and the force required to climb hills are all components of the road load. When all of these considerations are considered, the framework of the vehicle dynamics that govern the kinetics of the automobile as a whole can be characterized as [3, 13–16].

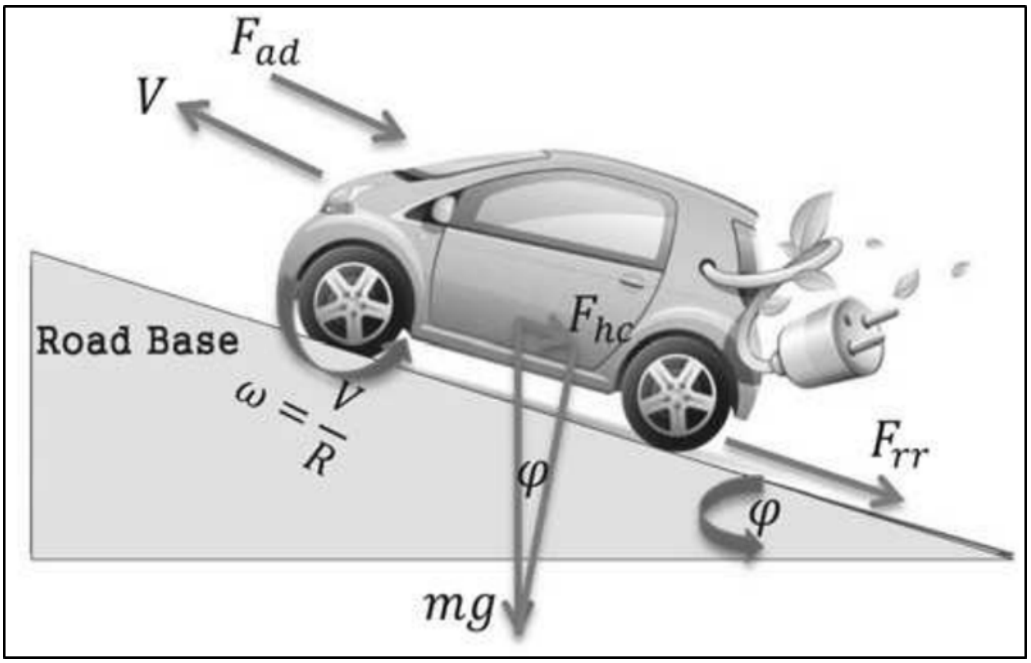

Figure 1: The fundamental layout of a compact electric vehicle [17]

$$F = \mu_{rr} mg + \frac{1}{2}\rho A C_d v^2 + mgsin(\varphi) + \frac{mdv}{dt} \quad (1)$$

Where the velocity of the EV is denoted by v, the head portion of the car or truck is represented by A, the electric vehicle mass corresponds to m, the rolling resistance coefficient is denoted by μ_{rr}, while g represents the acceleration gravity, the density of the air is denoted as ρ, moreover, φ represents the angle at which machine climbs a slope, in other words, φ stands for the climbing angle, and C_d is the coefficient of the drag operation, as listed in Table 1.

Table 1: System parameters as introduced in Equation 1

Symbol	Description
V	Velocity
A	Area
m	EV-mass
μ_{rr}	Rolling resistance
g	Acceleration
ρ	Density
φ	Climbing angle
C_d	Coefficient of drag

However, Equation 1 can be divided into four parts. That is, the first one is the force of the rolling resistance, $\mu_{rr}mg$, the next part stands for the drag-force of the aerodynamic system, $\frac{1}{2}\rho AC_d v^2$, the third part, $mgsin(\varphi)$, represents the force of the climbing, while the acceleration part is the last one in Equation 1, $\frac{mdv}{dt}$.

The consequent force (F) will result in a torque, counterproductive to the driving motor, as illustrated by the following formula [2].

$$T_L = F\left(\frac{r}{G}\right) \tag{2}$$

The gearing ratio is represented by *G*, while *r* stands for the radius of the EV tires. Moreover, the torque that will be produced by the EV-driving motor is T_L.

2.2 Modeling of The Electric Motor

The suggested EV system is driven by a DC motor, and the dynamics of the DC motor device are coupled to those of the EV scheme through a transmission unit. The non-linear concept of the DC motor can be demonstrated using the equations below [17]:

$$\frac{di}{dt} = \left(\frac{1}{L_a + L_{field}}\right) \times \left\{V - \left(R_a + R_f\right).i - L_{af}.i.\omega\right\}$$

$$\frac{d\omega}{dt} = \left(\frac{1}{J}\right) \times \left\{L_{af}.i^2 - B\omega - T_L\right\} \tag{3}$$

Where *i* is the current of the armature, *v* is the motor rotation speed, L_a denotes the inductance of the armature, R_a stands for the resistance due to the armature, while the resistance of the field winding is denoted by R_f, L_{field} represents the inductance of the field winding, the viscous coefficient is given as *B*, accordingly, the motor, which includes the transmission and the tires, has an inertia of *J*, further, the external torque corresponds to T_L, the input of voltage value to the system is denoted as *V*, thus, Saturation causes a non-linear impact on the presumed mutual inductance L_{af} between the field winding and the armature winding. Next, the relationship that exists between the angular speed of the motor and the driving velocity of the vehicle will be discussed. This relationship is denoted by the letter *v*, which can be calculated as,

$$v = \left(\frac{r}{G}\right)\omega \tag{4}$$

Where the angular angle is represented by ω.

2.3 Modeling of EV

By Combining the kinetic and electrical models, the following equation demonstrates literally the entire non-linear dynamic description of the EV:

$$\frac{di}{dt} = \left(\frac{1}{L_a + L_{field}}\right) \times \left\{V - \left(R_a + R_f\right).i - L_{af}.i.\omega\right\}$$

$$\frac{d\omega}{dt} = \left(\frac{1}{J + m(r/G)^2}\right) \times \left\{L_{af}.i^2 - B\omega - \left(\frac{r}{G}\right) \times \left(\mu_{rr}mg + \frac{1}{2}\rho AC_d v^2 + mgsin(\varphi)\right)\right\} \tag{5}$$

The control system for such structures should be developed using suitable non-linear control approaches. The wide range of process parameters causes some parameters to change, and making precise design a hard mission. For instance, the armature resistance of the motor is subject to change as the operating temperature varies. This highlights the significance of the controller's resilience. The parameters and coefficients of the EV used in this research are explained in Table 2. Without a controller, the speed response of the system (described by Equation 5) has suffered from high settling time (over 10 seconds)

and high steady-state error (over 35%), the speed response of the EV system is shown in Figure 2, Based on the above, high performance and the robust controller is needed.

Table 2: Non-linear EV system coefficients [17]

Symbol(s)	Quantities	Unit	Symbol(s)	Quantities	Unit
$R_a + R_f$	0.2	Ohm	A	1.8	m^2
$L_a + L_{field}$	6.008	mH	ρ	1.25	Kg/m^3
r	0.25	m	C_d	0.3	
J	0.05	g/cm^2	φ	0	
L_{af}	1.776	mH	μ_{rr}	0.015	
V	0-48	V	G	11	
I	78	A	B	0.0002	N*m/(rad/s)
m	500	Kg			

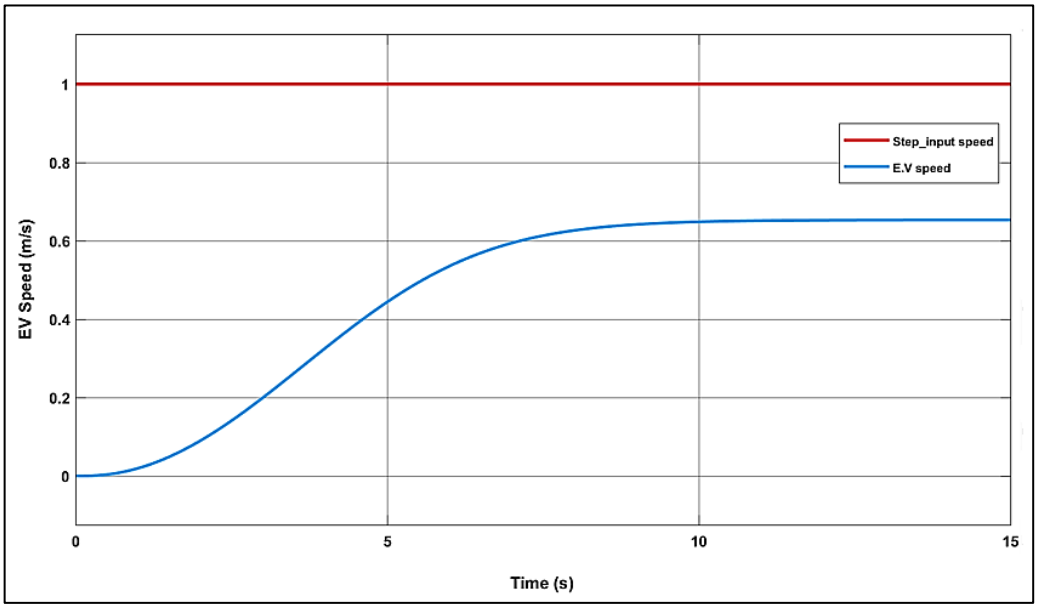

Figure 2: The response EV model without controller

3. PID Controller

The PID-controller is a common example of an older style of controller. Input voltage r(t) is compared to output speed y(t) to get the monitoring error e(t). The PID controller will then take e(t) as input. In the time domain, the equation for the control signal looks like this:

$$\mathrm{U}(t) = K_P e(t) + K_i \int_0^t e(t)\,dt + K_d \frac{de(t)}{dt} \tag{6}$$

Following the application of the Laplace transform to both sides of the equation presented earlier and the subsequent reordering of the resultant expression, the function generator of the PID controller may be expressed as follows:

$$\frac{u(s)}{e(s)} = K_p + \frac{K_i}{s} + K_d s \tag{7}$$

Where the proportional gain is K_p, and the integral gain is represented by K_i while K_d stands for the derivative gain [18]. PSO and MVO are two of the numerous ways that may be utilized to adjust the controller's settings; however, we will only be utilizing PSO and MVO for the sake of this particular study.

4. Optimization Algorithms

Population-based optimization algorithms, also known as metaheuristic optimization algorithms, are a type of stochastic algorithm that is used in resolving optimization problems. These techniques make use of several agents, or solutions, in order to travel across the search space. This section provides examples of two of these strategies, namely the PSO and MVO algorithm families.

4.1 Particle Swarm Optimization

It is one of the population-based algorithms that use population of particles, each of them translates an elect random decision. It was invented by Eberhart and Kennedy in 1995. The benefits of population-based methods can be able to optimize variable problems in a continuous or discrete form. They are free of derivative information. They have able to find solution in a large boundary of the objective function areas at the same time. They can be used in parallel computations. Also, they can eliminate the local minimum trapping and they can give many suitable parameters for multimodal issues. In PSO, a swarm of particles is first generated by assigning a completely arbitrary position and speed to each individual particle in the group. These particles are placed in the entire exploration space of a number of different functions or compounds. These particles are responsible for determining the cost function, and the personal best of each particle is stored in the Pbest variable, while the global best of the entire swarm is stored in the Gbest variable. By using Equation (8) and Equation (9), these particles will be moved to new locations in the subsequent iteration. The individual best and the globally best locations are sent to each particle, and from there, the particles gradually move closer and closer to the global best locations. This process is repeated until all of the swarm's particles will eventually meet at the same spot, either until the maximum number of iterations has been reached, at which point the best individual best particle will have been determined through the application of the computation of the fitness function [19]. PSO may be understood by referring to the two expressions that describe how the speed and location of each particle are updated [20]:

$$v_{i+1} = w * v_i + c_1 r_1 (pbest - x_i) + c_2 r_2 (Gbest - x_i) \quad (8)$$

$$x_{i+1} = x_i + v_{i+1} \quad (9)$$

Where c_1 and c_2 describe the individual and group learning rates, respectively, and r_1 and r_2 are utilized as randomized values in the range [0-1]. The values of the variables c_1 and c_2 show the relative relevance of the particle's best position in comparison to the best place of its neighbor. *w* is the inertia weight factor that is used to improve the search stability; pbest and Gbest describe the personal and global best particle places, respectively, in the swarm; and w is the inertia weight factor. The velocity of the particles are slowed down using w in order to improve the level of precision and accuracy with which they can locate the ideal solution. When trying to increase the global search activity of the swarm, a bigger value of w is used, whereas when trying to increase the local search activity, a lower value of w is used [21].The flowchart for the PSO is given in Figure 3.

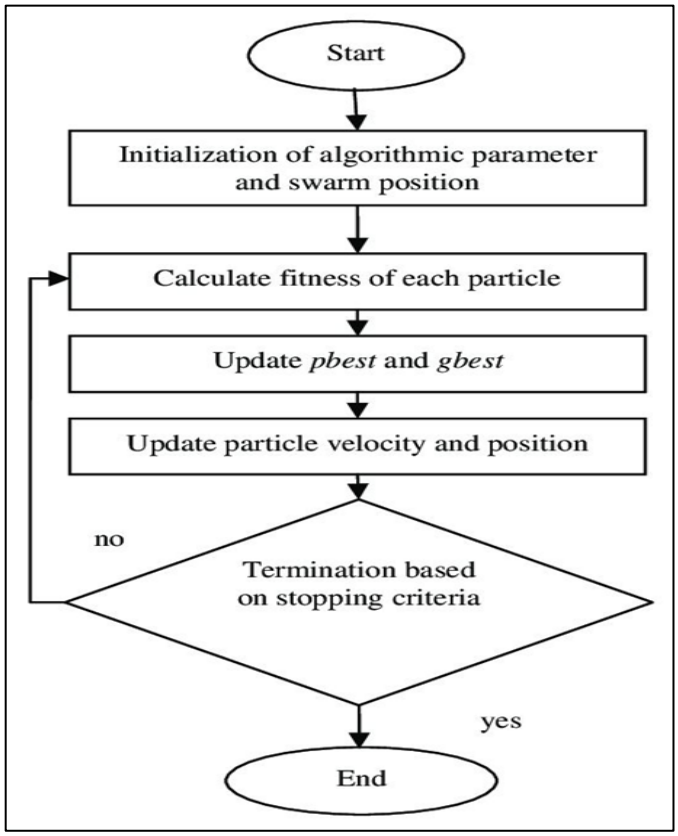

Figure 3: Flowchart of the PSO algorithm

4.2 Multi-Verse Optimization Algorithm

A group of scientists came up with the multi-verse theory, and the multi-verse view of the universe (MVO) is based on this idea. It is generally accepted that there was more than one big bang, and the fact that there are several universes that arose from each of these events indicates that there must have been more than one big bang. In addition to this, in accordance with the theory that posits the origin of the cosmos. The premise that underpins this theory is that the universe in question is its antithesis. According to this model, the universes in question may either interact with one another or even crash with one to another [22]. The multi-verse optimization technique is founded on three key notions from the field of cosmology: wormholes, black holes, and white holes [23]. According to the findings of physicists, the white hole, which is synonymous with the term "big bang", is the primary factor in the beginning of the universe. It came into existence after the collision of two different universes in parallel. Because of their incredibly strong gravitational pull, black holes grab all, even light beams. Black holes are the opposite of white holes, which are also known as singularities. Wormholes are like time and space highways in which items are able to move instantaneously between two distinct points of a universe or even between two separate worlds. Wormholes may also be used to connect two different locations in the same universe. MVO essentially converges on the objective by transmitting and acquiring entities (factors) across universes, which causes the goal to converge (solutions). This transmitting and receiving mechanism is reliant on the inflationary pressures of the universes, also known as their fitness values, which are computed through a sequence of iterations. When a universe has a high inflation rate, it has a high probability of containing white holes and has a tendency to send objects in the direction of other universes. If the rate of inflation in a universe is low, then that universe very certainly contains a black hole and is more likely to take in foreign items. This procedure, which is referred to as the exploration stage of the procedure, is modeled algebraic equation:

$$U = \begin{bmatrix} x_1^1 & x_1^2 & \cdots & x_1^p \\ \vdots & \vdots & \vdots & \vdots \\ x_n^1 & x_n^2 & \cdots & x_n^p \end{bmatrix}, \quad x_i^j = \begin{cases} x_k^j, & r_1 < NI(U_i), \\ x_i^j, & otherwise, \end{cases} \tag{10}$$

Where U_i represents the i-th universe, p represents the number of characteristics, n corresponds to the number of universes, x_i^j represents the j-th attribute of the i-th universe, r_1 is a random number in the range [0, 1], $NI(U_i)$ represents the normalized inflation rate of the i-th universe, and x_k^j represents the j-th attribute of the selection process consisting of a roulette wheel was used to choose the k-th universe.

During the exploitation stage of the process, it is supposed that every universe makes use of wormholes in order to transport things through space in a random pattern, irrespective of the inflation rate. Wormholes are also utilized to execute localized modifications within every universe by creating a link to the solution space that has been established so far. This is done by connecting to the solution space. The workings of this system can be summarized as one mathematical expression:

$$x_i^j = \begin{cases} \begin{cases} X_j + TDR \times \left((ub_j - lb_j) \times r_4 + lb_j \right) r_3 < 0.5 \\ X_j - TDR \times \left((ub_j - lb_j) \times r_4 + lb_j \right) r_3 \geq 0.5 \end{cases}, & r_2 < WEP, \\ x_i^j, & r_2 \geq WEP, \end{cases} \tag{11}$$

Where X_j is the j-th parameter of the best universe produced so far, r_2, r_3, and r_4 are uniformly distributed random values in [0, 1], while ub_j and lb_j are being utilized to establish the minimum and maximum values of the j-th factor. The *WEP* and *TDR* parameters are going to be discussed further down in this article. The likelihood that a wormhole actually exists somewhere in the cosmos is denoted by the acronym *WEP*. To put more of an emphasis on exploitation, the technique linearly raises this parameter as the number of repeats increases. The following is the formula used to compute *WEP*:

$$WEP = min + l \times \left(\frac{max - min}{L} \right) \tag{12}$$

Where the minimum (*min*) is set at 0.2 and the maximum (*max*) at 1. Maximum iteration value (L) is displayed with the current iteration step (l). *TDR*, or the Touring Distance Rate, is another factor. It's what you need when you're sending things throughout a wormhole to the most ideal world discovered so far. Eq. (13) provides the formula for *TDR*:

$$TDR = 1 - \frac{l^{(1/p)}}{L^{(1/p)}} \tag{13}$$

whereas p is an indicator of the exploitation precision and the primary key for it is set to 6 [23]. The flowchart for the MVO is given in Figure 4.

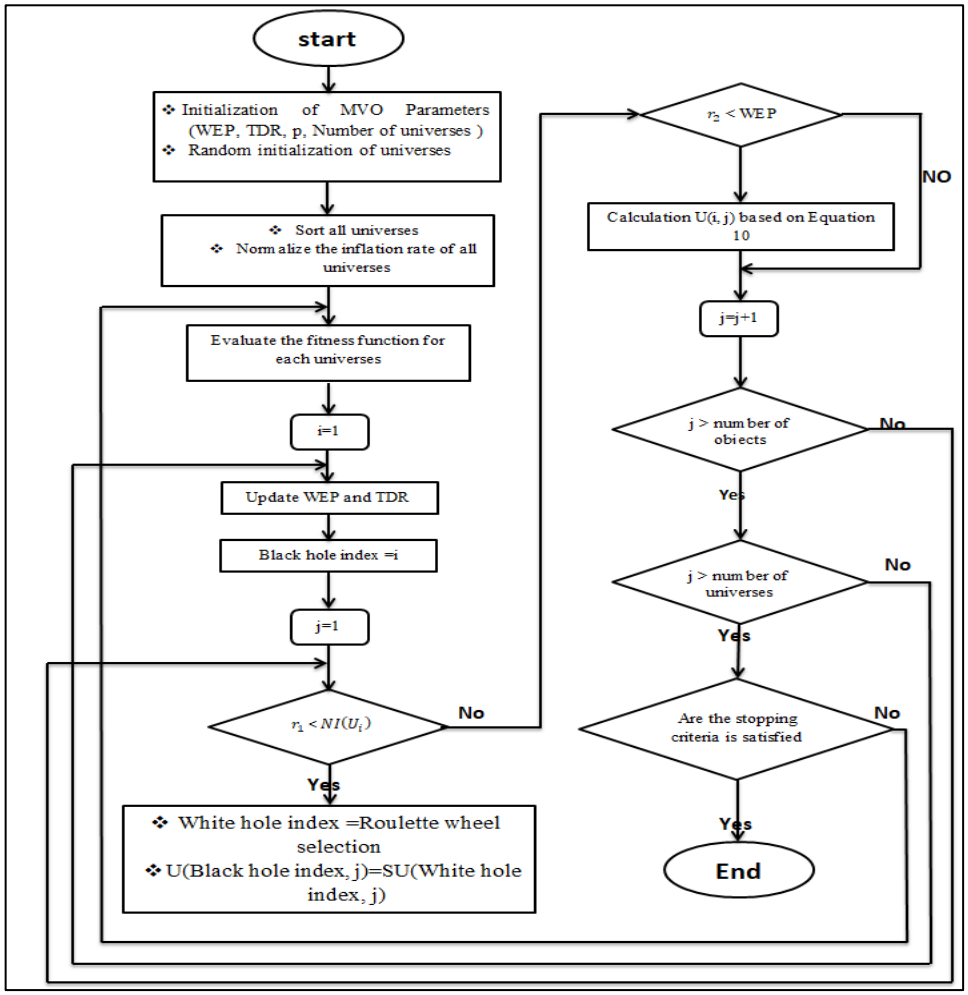

Figure 4: Flowchart of the MVO algorithm

5. Discussion of Results and Simulation

The proposed controller is simulated in MATLAB 2020a. A PC with core i7 processor at 2.40 GHz with 8 GB of RAM is utilized, and the operating system is Windows 10. In this paper PSO and MVO algorithms are used to tune the parameters of the PID controllers to reach the optimal response with minimum tracking error. The application of PSO and MVO algorithms needs to define the cost function. In this research, ITSE (Integral Time-weighted Squared Error) cost function is used, ITSE is described by the following Equation:

$$Fitness = ITSE = \int_0^t t * Eror(t)^2 \quad (14)$$

Here, *Error* represents the discrepancy between the target and the actual velocity of the EV. Figure 5 shows the Simulink diagram of the proportional-integral-derivative (PID) controller applied to the EV model.

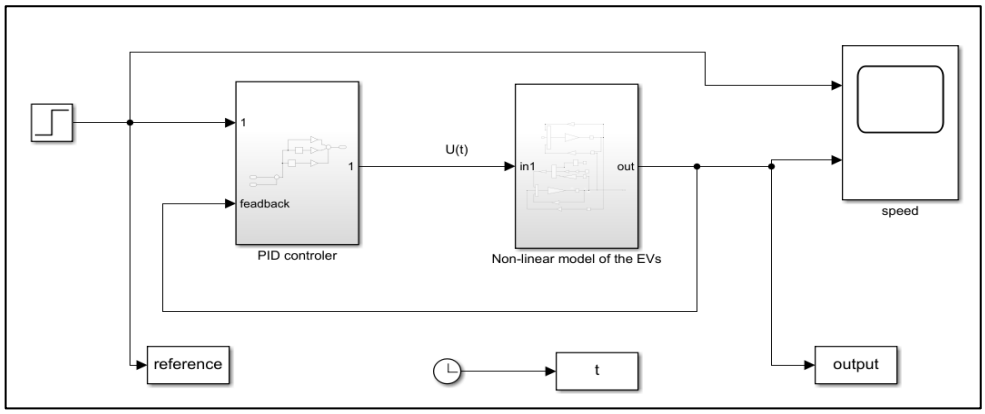

Figure 5: Non-linear exemplary of the EVs speed control simulation with PID controller

The parameters of the PSO and MVO are given in Table 3, the proposed controllers are tested by both linear (step), and nonlinear (sine wave) disturbances.

Table 3: The parameters of PSO and MVO algorithms

Parameters	Selected values of PSO	Selected values of MVO
No. of iterations (N_i)	50	50
No. of search agents/universes (n)	10	5
No. of variables (Dim)	3	3
Lower bound (lb)	[10 5 0.1]	[10 5 0.1]
Upper bound (ub)	[40 15 10]	[40 15 10]

The optimum parameters of the PID controller by using PSO and MVO algorithms are given in Table 4.

Table 4: The optimal parameters of the PID Controller

PID Controller parameters	Values	
	PSO	MVO
K_p	31.8552	40.000
K_i	15.0000	15.000
K_d	2.6052	3.46787

5.1 Simulation Results of the Linear Trajectory

PSO-PID and MVO-PID controllers for EV systems have been evaluated by using a fixed input signal to analyze the step response of the entire system. Figure 6 displays the results of the step input test. A comparison between the two types of PID controllers is shown in Table 5. These results show that the PID controller with MVO improved speed response (small settling time ts), zero error steady state and minimum or no oscillation (maximum peak M_P< 5%), compared with PSO–PID that has higher oscillation (maximum overshot $M_P > 25\%$).

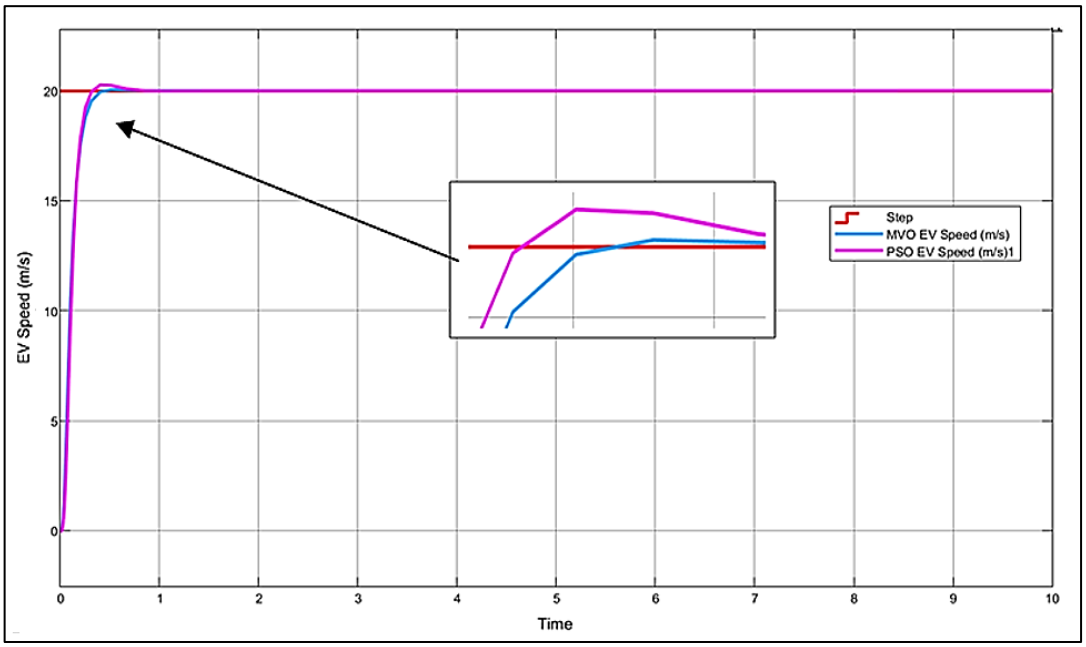

Figure 6: Speed control response with PID controllers and PSO and MVO optimization

Table 5: Comparison between the performances of PSO-PID and MVO-PID controllers

Speed controller	Maximum overshoot M_P (%)	Delay time t_d(sec)	Peak time t_p(sec)	settling time t_S (sec.)	rising time t_r (sec.)	steady state error
PSO-PID	0.25	0.11	0.441	0.767	0.211	Approaches to zero
MVO-PID	0.05	0.11	0.528	0.807	0.215	Approaches to zero

5.2 Simulation Results of the Non-linear Trajectory

The results of this test are displayed in Figure 7. The results show that the proposed two controllers are accurate and have fast responses in tracking the speed of the vehicle to the desired speed. In other words, the speed deviation between the actual and the desired is negligible with no increase in the steady-state error than the step input test. The obtained results for linear and nonlinear paths illustrate that the proposed PID controllers is efficient in controlling the electric vehicle.

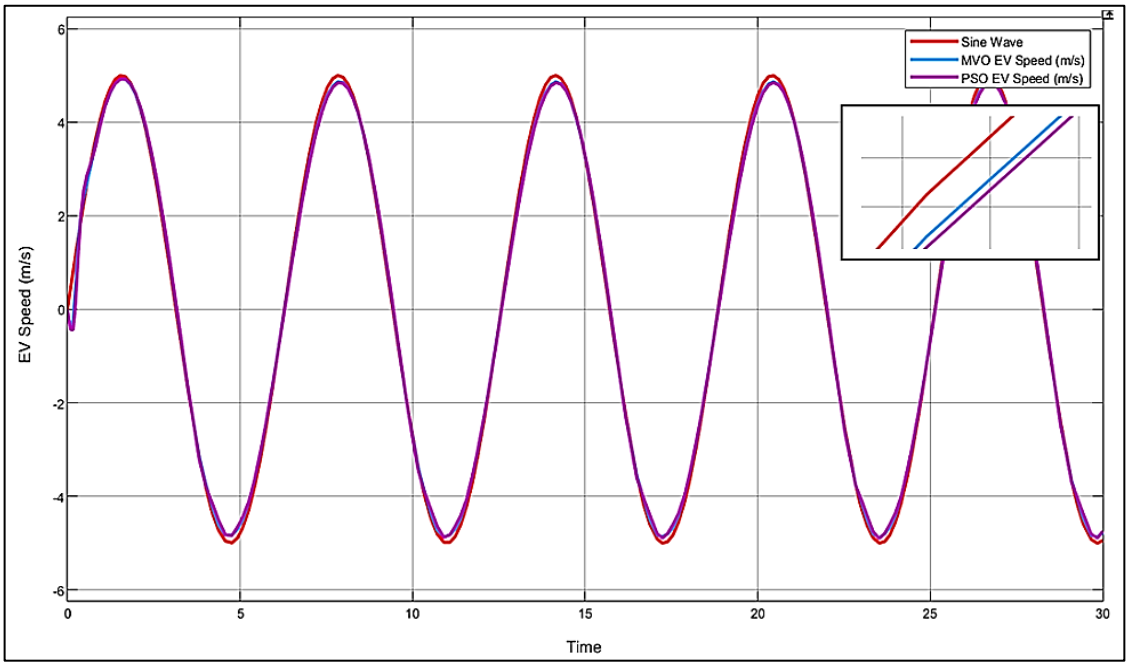

Figure 7: Speed control response with PID controllers and PSO and MVO optimization

6. Conclusion

The objective of this paper is to develop a Proportional-Integral-Derivative (PID) controller as a speed controller for an electric vehicle. Two methods were used to optimize the parameters of the PID, which are particle swarm optimization and multi-verse optimization. The nonlinear trajectory test demonstrates that MVO-PID controller attained lower error as compared to the PSO-PID controller. The simulation results of the linear trajectory test show that the MVO-PID controller has less overshoot than PSO-PID. Settling time and rising time obtained by PSO-PID controller are 0.767s and 0.211s, respectively, while by MVO–PID controller are 0.807s and 0.215s, respectively. Thus, the results illustrate that the two control systems, proposed in this work, are efficient in controlling the electric vehicle, it can be considered that MVO-PID is the better of the two controllers. The work can be further developed in the future by using anther motors for the electric vehicle system instead of DC motors such as induction motor, brushless DC motors , etc. as well as it can be applied using FPGA technology or any other technology.

Author contribution

The contribution of authors is as follows: Conceptualization, simulation and writing, Arkan A. Jassim; supervision and result analysis, Ekhlas H. Karam; supervision and proof read of the manuscript, Mohammed Moanes E. Ali

Funding

This research work has no support funding

Data availability statement

The data that support the findings of this study are available on request from the corresponding author.

Conflicts of interest

There is no conflicts of interest

References

[1] C.H. Chiu and, Y.T. Hung,bOne wheel vehicle real-world control based on interval type 2 fuzzy controller, Elsevier, Mechatronics, 70 (2020) 102387.https://doi.org/10.1016/j.mechatronics.2020.102387

[2] F. Hacker, R. Harthan,F. Matthes, W. Zimmer, Environmental impacts and impact on the electricity market of a large scale introduction of electric cars in Europe – criticalreview of literature, ETC/ACC technical paper .4 (2009) 56–90.

[3] A. Artmeier, J. Haselmayr, M. Leucker, M.Sachenbacher, The shortestpath problem revisited: optimal routing for electric vehicles" In: Dillmann K, Beyerer J, Hanebeck UD, et al. (eds) KI 2010: advances in artificial intelligence. Berlin: Springer, 6359,2010, 309–316. https://doi.org/10.1007/978-3-642-16111-7_35

[4] S. Kaushik,Electric Vehicles: Review On Current Trends, Potential And Challenges, Sch. Res. J. Interdiscip. Stud., Peer Rev.Referred J., (2019) 12184-12189.

[5] F.J. Daya, P. Sanjeevikumar, F. Blaabjerg, P. W. Wheeler, J. O. Ojo, A. H. Ertas, Analysis of wavelet controller for robustness in electronic differential of electric vehicles: an investigation and numerical developments, Electr. Power Compon. Syst., 44 (2016).763–773.https://doi.org/10.1080/15325008.2015.1131771

[6] A. Raisemche, M. Boukhnifer, C. Larouci., D. Diallo,Two active fault-tolerant control schemes of induction-motor drive in EV or HEV, IEEE Trans. Veh. Technol., 63 (2014) 19–29. https://doi.org/10.1109/TVT.2013.2272182

[7] X. J. Jin, G. Yin and, N. Chen, Gain-scheduled robust control for lateral stability of four-wheel independent- drive electric vehicles via linear parameter-varying technique, Elsevier, Mechatronics, 2015. https://doi.org/10.1016/j.mechatronics.2014.12.008

[8] A. Pakniyat and, P. E. Caines, Hybrid optimal control of an electric vehicle with a dual-planetary transmission, Elsevier, Nonlinear Analysis: Hybrid Systems, 2016. http://dx.doi.org/10.1016/j.isatra.2016.04.019

[9] N. K. Saxena, S. Gebrehiwot and, D. Mena, Controller Design for Electric Motor Derived Vehicle, Indonesian Journal of Electrical Engineering and Informatics (IJEEI), 6 (2018) 125-131. http://dx.doi.org/10.52549/ijeei.v6i2.282

[10] Z. Wang, U. Montanaro, S. Fallaha,A. Sorniottia , B.LenzoA gain scheduled robust linear quadratic regulator for vehicle direct yaw moment Control, Elsevier, Mechatronics, 51 (2018) 31-45. https://doi.org/10.1016/j.mechatronics.2018.01.013

[11] J. J. Makrygiorgou, A. T. Alexandridis, Power Electronic Control Design for Stable EV Motor and Battery Operation during a Route, MDPI, Energies, 2019.https://doi.org/10.3390/en12101990

[12] K. A. Nitesh , Ravichandra, A Study on Battery Controller Design for the Estimation of State of Charge (SoC) in Battery Management System for Electric Vehicle (EV)/Hybrid EV (HEV), SN COMPUT. SCI., 197 (2021). https://doi.org/10.1007/s42979-021-00600-0

[13] J. Larminie, J. Lowry,: Front matter (John Wiley & Sons, Ltd, 2003).

[14] M.H. Khooban, , N. Vafamand, T. Niknam, T–S fuzzy model predictive speed control of electrical vehicles, ISA Trans., 64 (2016) 231–240.https://doi.org/10.1016/j.isatra.2016.04.019

[15] Q. Huang, Z. Huang, H. Zhou, Nonlinear optimal and robust speed control for a light-weighted all-electric vehicle, IET Control Theory Appl.3 (2009) 437–444 https://doi.org/10.1049/iet-cta.2007.0367

[16] M.H. Khooban, O. Naghash-Almasi, T. Niknam, M. Sha-Sadeghi1, Intelligent robust PI adaptive control strategy for speed control of EV(s), IET Sci. Meas. Technol., 10 (2016) 433–441.https://doi.org/10.1049/iet-smt.2015.0190

[17] H.K. Mohammad , V. Navid, T. Niknam, T. Dragicevic,Model-predictive control based on Takagi-Sugeno fuzzy model for electrical vehicles delayed model" IET Electr. Power Appl., 11 (2017) 918–934. https://doi.org/10.1049/iet-epa.2016.0508

[18] G. Y . Mustafa., A. T. Ali, E. Bashier, M. F. Elrahman, Neuro-Fuzzy Controller Design for a Dc Motor Drive, University of Khartoum Eng. J., (UofKEJ), 3 (2013) 7-11.

[19] D. Wang , D.Tan and L.Liu, Particle Swarm Optimization Algorithm: an Overview, Soft Computing, Springer, 22 (2018) 387-408. http://dx.doi.org/10.1007/s00500-016-2474-6

[20] M. Malathi, K. Ramar, C. Paramasivam and M. Malathi, Optimal Path Planning for Mobile Robots using Particle Swarm Optimization and Dijkstra Algorithm with Performance Comparison, Middle East J. Sci. Res., 24 (2016) 312-320. https://doi.10.5829/idosi.mejsr.2016.24.S1.65

[21] J. Sun , C. Hong Lai and X. Jun Wu, Particle Swarm Optimization Classical and Quantum Perspectives, CRC Press, Taylor & Francis Group, London, 2012.

[22] A. E. Taser, K. Guney, E. Kurt, Circular Antenna Array Synthesis Using Multiverse Optimizer, Int. J. Antennas Propag.,. March, 2020 (2020). https://doi.org/10.1155/2020/3149826

[23] S.Mirjalili, S. M. Mirjalili, A. Hatamlou, Multi-Verse Optimizer: a Nature-Inspired Algorithm for Global Optimization, Neural Comput. Appl., 27 (2015) 495–513.http://dx.doi.org/10.1007/s00521-015-1870-7.